GRAFTING POLYMERS TO SINGLE-WALLED CARBON NANOTUBES

By

XIAOMING JIANG

Master of Engineering

Nanjing University of Technology

Nanjing, China

2002

Submitted to the Faculty of the
Graduate College of the
Oklahoma State University
in partial fulfillment of
the requirements for
the Degree of
MASTER OF SCIENCE
July, 2005

GRAFTING POLYMERS TO SINGLE-WALLED

CARBON NANOTUBES

Thesis Approved:

Thesis Adviser

Dean of the Graduate College

PREFACE

Single-walled carbon nanotubes (SWNT) are seamless cylinders derived from graphite sheets. Due to the strong interaction among bundle structures, the nanotubes pack into big bundles and have poor solubility in various solvents, which is a big hindrance for further applications of SWNT.

A polymer is a very large chain-like molecule formed by combining a large number of smaller molecules together. Plastics, fibers, rubbers, and adhesives are made from polymers. We attached polymers to sidewalls or ends of SWNT to break big bundles into small bundles and prepare stable black solutions. The attached polymers wind around the SWNT and peel off the aggregated tubes under stirring or sonication.

We successfully attached four kinds of polymers to SWNT and obtained black solutions, respectively. Characterization by microscopy shows that SWNT bundles were broken into small ones, and spectroscopy shows that chemical bonds were formed between SWNT and polymer chains.

ACKNOWLEDGEMENTS

I would like to express appreciation to my research advisor Dr. Warren T. Ford, for his guidance and support. I am very grateful to Dr. Berlin and Dr. Slaughter serving in my advisor committee. Thanks for my research colleagues, Dr. Qin Shuihui, Dr. Tan Susheng, Mr. Maxim Tchoul, and Ms. Young Hie Kim, for their help and encouragement.

I owe my parents too much, which is far beyond my gratitude.

Thanks for Charles Hunt and Chuck Blackledge in Department of Physics for technique support.

Finally I would like to thank for Department of Chemistry of Oklahoma State University for financial support.

TABLE OF CONTENTS

LIST OF TABLES

LIST OF FIGURES

CHAPTER I

CHAPTER III

CHAPTER I

INTRODUCTION

Discovery. Carbon nanotubes were discovered by Japanese electron microscopist Sumio Iijima in 1991. When he was studying the fullerenes from an arc discharge process, he found multiwall carbon nanotubes in the carbon sooton the negative electrode.[1] The transmission electron microscopy (TEM) image of the mutiwall carbon nanotubes he observed shows special structures as seamless cylinders derived from a graphene sheet shown in Figure 1.[2] In 1993, single-walled carbon nanotubes (SWNT) were discovered independently by Bethune[3] and Iijima.[4] The typical images of SWNT were shown in Figure 2.[5]

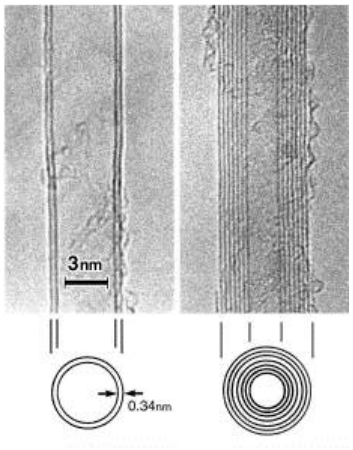

Figure 1. Multi-wall carbon nanotubes discovered in 1991.[2]

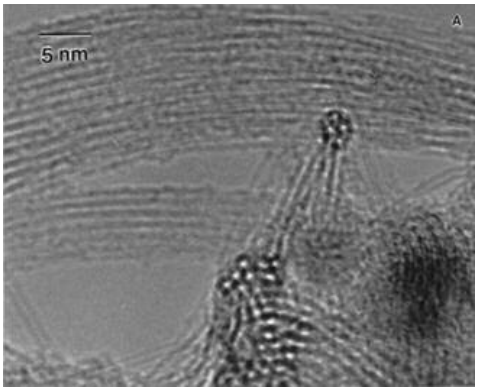

Figure 2. High resolution TEM image of ropes of SWNT produced in the arc using Ni- Y catalyst.[5]

Synthesis. Carbon nanotubes can be synthesized by several routes such as chemical vapor deposition (CVD), arc-discharge, and pulsed laser vaporization. CVD is a general chemical process to produce solid material on certain substrates by feeding volatile precursors. In CVD, nanotubes grow from the catalyst island on the substrate with the hydrocarbon as the feedstock. Although the CVD method only requires relatively low temperature (550~750 °C),larger quanti ty of defects were found in the sidewall structure than from other methods. In pulsed laser vaporization nanotubes are produced by vaporizing the surface of carbon target with a high-energy laser and then condensing vapor on a substrate. In arc discharge, nanotubes are produced from the condensation of carbon vapor created by arc discharge between two carbon electrodes.[6] Both arc discharge and laser vaporization require a carbon source at • 3000 °C, which is not so efficient.[7]

Another milestone in synthesis of nanotubes is the research carried by Smalley's group in 1999. They developed the high pressure CO disproportion process (HiPco), a

technique for production of SWNT by using CO as carbon feedstock and $Fe(CO)_5$ as catalyst. Size and diameter distribution can be roughly selected by controlling the pressure. The process paved the way for the bulk production of carbon nanotubes.[8]

Resasco developed a "controlled production" of single-walled carbon nanotubes by Co–Mo/SiO_2 catalyst. The CO was introduced at 700 ºC in a horizontal quartz tubular reactor after the reactor was heated to 500 ºC by H_2 and then 700 ºC by He. SWNT were produced in large quantities, most of them aligned as bundles. Smaller quantities of defects and amorphous carbon were found in the samples compared with the pulsed laser vaporization and arc discharge methods.[9]

Properties. The seamless-cylinder structure of carbon nanotubes gives nanotubes special mechanical, thermal and electronic properties.

Nanotubes can be defined by a chiral vector $\mathbf{C}_h$ and a chiral angle θ.

$\mathbf{C}_h = n\mathbf{a}_1 + m\mathbf{a}_2$ where a_1 and a_2 are lattice vectors, shown in Figure 3.

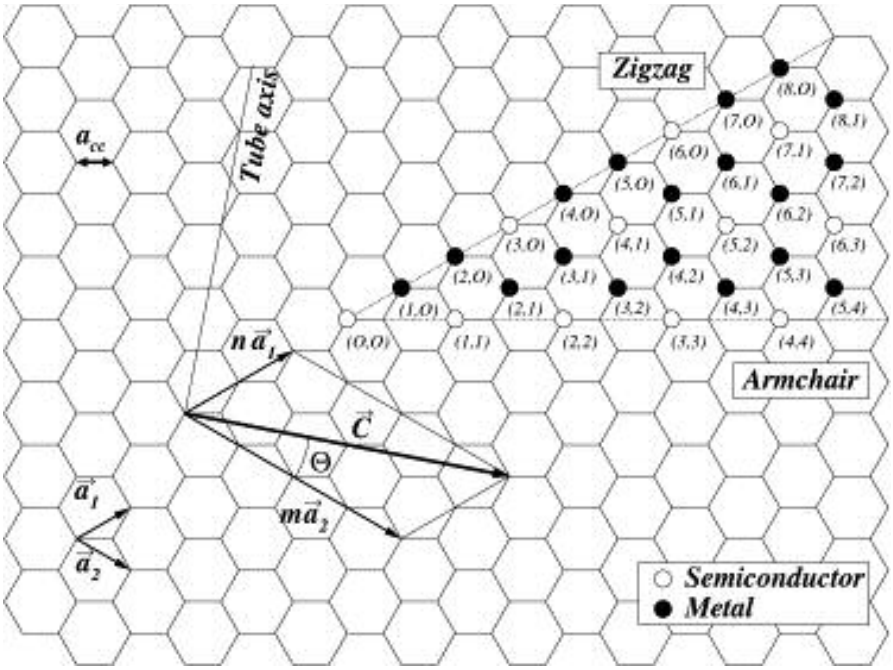

Figure 3. 2D graphene sheet showing chiral vector Ch and chiral angle .[10]

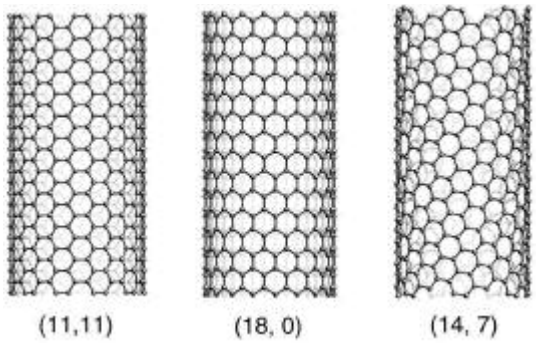

Figure 4. Computer generated images of single-wall carbon nanotubes:
(a) (11,11) armchair type, (b) (18,0) zig-zag type, and (c) (14,7) helical type.[2]

When n = m, the nanotubes are armchair ($\theta = 0^o$); when m = 0, nanotubes are zigzag ($\theta = 30^o$), shown in Figure 4. With $|n-m| = 3q$, nanotubes are metallic while with $|n-m| = 3q \pm 1$, nanotubes are semiconducting (q is integer).[10]

Electronic properties of a nanotube are owing to its unique one-dimensional structure which yields quantum confinement of electrons normal to the nanotube axis. The function of energy, density of states (DOS) of nanotubes, was characterized by a number of singularities shown in Figure 5. Semiconducting nanotubes differs from

metallic nanotubes by the energy gap between the valence band and the conduction band.[7]

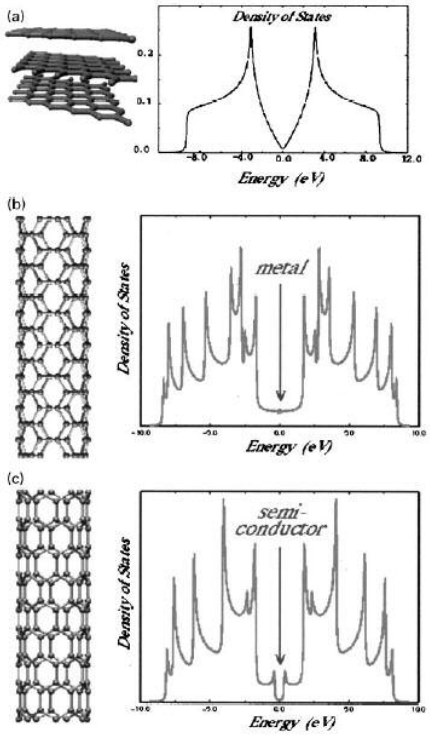

Figure 5. Density of states of graphite, metallic tubes and semiconducting tubes**:** a) graphite, semimetal small overlap between valence and conduction band; b) metallic armchair (5,5) tube which shows electronic states at the Fermi energy E_f (characteristic of a metal); c) zigzag tube (7,0) revealing semiconducting behaviour caused by energy gap located between valence and conduction band (characteristic of semiconductors). Density of states (DOS), exhibiting valence (negative values), conduction band (positive values), and Fermi energy (E_f; centered at 0 eV) for graphite and metallic armchair and zigzag tubes: spikes shown in DOS of tubules are called 'van Hove' singularities and are due to one-dimensional quantum conduction, which is not present in an infinite graphite crystal.[6]

The mechanical properties of carbon nanotubes are due to their strong carbon-carbon covalent bonding and their van der Waals force among bundle structures. Strong chemical bonds and interactions between tubes can consume a lot of energy. The Young's modulus of carbon nanotubes reaches ~810 GPa from the AFM technique for characterization of SWNT bundles, while Young's modulus of steel is 208 GPa. In addition, a SWNT is flexible and can be twisted or bent.[7]

The thermal properties of carbon nanotubes are due to nanotube lattice vibrations, "the phonons".[7] The Biercuk group studied thermal conductivity of SWNT/epoxy composites. Samples loaded with 1 wt% of unpurified SWNT showed a 70% increase in

the thermal conductivity at 40 K and 125% increase at room temperature, while enhancement from samples loaded with carbon fibers was three times smaller.[11]

Applications. SWNT are exploited to prepare field emission instruments, lithium ion batteries, biomedical delivery vessels, molecular sensors, and nanoelectronic devices by taking advantage of their unique electronic, mechanical and thermal properties.

1. Field Emission Sources. Field emission is the extraction of electrons from a solid by tunneling through the surface potential surface. Electrons can be emitted from carbon nanotubes because they have a high ratio of length/diameter and high conductivities. The idea was employed in nanotube flat-panel displays, which were proposed in 1995 and realized three years later.[6]

2. Lithium Ion Batteries. Li-ion batteries are used as power source in cell phones and laptops. Carbon nanotubes were applied in Li-ion batteries as anodes, which will intercalate the ions. Nanotubes have more storage potential due to the conductivity and special surface area for Li ions compared with regular graphite.[6]

3. Biomedical Delivery. Once the sidewalls of nanotubes were functionalized, the solubility was improved, which made it possible for nanotubes to be further functionalized by drugs, antigens, and genes. Solubility in aqueous solution and cationic surfaces of functionalized carbon nanotubes (CNT) enable the nanotubes to cross the plasma membrane and distribute through the cellular compartments.[12]

4. Molecular Sensors. The absorption of some gases by bundles of nanotubes will result in an electron transport change in the SWNT materials. This feature could be employed to prepare some gas sensors in a chemical plant for detecting the leakage of toxic gases.[6]

5. Nano Electronic Devices. Various kinds of transistors, as well as logic gates and logic rings, were fabricated from nanotubes. The semiconducting tubes with its special bandgap are building blocks for the nanoelectronic devices.[6]

Chemical Modification of SWNT

1. Oxidation of SWNT. Oxidation can serve three purposes: 1) Oxidation removes impurities, such as amorphous carbon and catalytic metals which are produced in the synthesis of carbon nanotubes. 2) Oxidation usually concurs with chemical cutting. Many applications require short nanotubes; for example, some electronic devices need SWNT with a certain band gap and precise length in specific locations. 3) Oxidation also provides active sites such as carboxylic acid groups on the sidewalls and ends of carbon nanotubes.

Gas phase oxidation is a common way to oxidize carbon nanotubes. A sample can be placed in a pure oxygen atmosphere and heated at desired temperature. Nagasawa and coworkers found at high temperature (500 °C) that SWNT will be gasified while catalytic particles and large graphite remained.[13] Gajewski and coworkers heated the SWNT samples in ceramic container under synthetic air flow, followed by washing with concentrated HCl to remove metal particles. Results show that amorphous carbon can be removed by this process due to its lower oxidative stability than SWNT, but graphite carbons such as C_{60} are unable to be removed.[14]

Typical acid oxidation was carried in concentrated acid, such as HNO_3 and H_2SO_4, or some mixtures of acids with H_2O_2. The Smalley group used HNO_3 as the oxidant to break the bundles of SWNT, cut them into short length, and introduce carboxylic acid

groups as well. Mild concentrated acid (5 M and 2.6 M) and long time processing (45 h) are required.[15-17]

A microwave air oxidation process was developed by Prato group, which involved short time (5 min) irradiation and followed by a wash with concentrated HCl to remove oxidized iron particles. This simple method was distinguished on removing catalytic iron particles in HiPco tubes.[18]

2. Common SWNT Sidewall Functionalization. Low solubility of carbon nanotubes in solvents is a hindrance for the application of SWNT. Functionalization of SWNT will introduce various functional groups along the ends and sidewalls of SWNT, which help break down the large bundles to single tubes or small bundles to give a stable solution. The electrostatic forces among those functional groups counterbalance van der Waals force among the bundles.

Addition reactions are the common way to add functional groups to the SWNT in which active species such as radicals, atoms, carbenes or nitrenes are required.

Fluorination of SWNT is obtained by treating pure SWNT with elemental fluorine at an elevated temperature (>150 ºC).[19] Although after fluorination, the electronic properties of SWNT were changed drastically, the fluorinated SWNT were able to be dispersed in alcohols. This solubility of SWNT enables further functionalization of SWNT through nucleophilic substitution reactions. Alcohols, amines, Grignard reagents, and alkyl lithium reagents were reacted with fluorinated SWNT to attach different groups to the sidewalls of SWNT. Therefore, fluorinated SWNT can act as intermediate species for further processes.[20]

Arylation of SWNT was obtained by adding arene diazonium salts to surfactant coated carbon nanotubes. The diazonium salts received an electron from the nanotubes,

and then ejected N_2 to form aryl radicals which reacted with sidewall of CNT. TGA analysis shows about 1 in 10 carbons on the sidewalls functionalized by aryl groups.[21]

Some other processes were applied to functionalize SWNT. Billups and coworkers prepared lithiated SWNT through reaction of SWNT with lithium metal in liquid ammonia. The lithiated SWNT can be materials for batteries and related storage applications.[22] Prato and coworkers developed another method involving 1,3-dipolar cycloaddition of an azomethine ylide to the sidewall of carbon nanotubes.[23] The Hirsh group worked on nitrene functionalized SWNT to attach alkyl chains, aromatic groups, dendrimers, crown ethers, and oligo(ethylene glycol) to SWNT. The research shows increment of intensity of D band in Raman spectroscopy is related to different degree of functionalization.[24] The Bingel reaction is another kind of cycloaddition reaction to cyclopropanate SWNT.[25]

3. Polymer Functionalization of Sidewall of SWNT. Physical absorption of a polymer to nanotubes was obtained by mixing polymer with nanotubes in certain solvents by heavy sonication or high shear mixing. Polymer functionalization of SWNT was first published by the Smalley group, who solublized SWNT in water by non-covalent association poly(vinyl pyrrolidone) (PVP) or polystyrene sulfonate with SWNT. Smalley provided a way to de-bundle the SWNT big bundles to generate small bundles so that the solubility of SWNT in aqueous solution was increased by interactions between polymer chains and sidewalls of SWNT.[26]

Covalent functionalization of nanotubes renders stronger interactions between polymer and nanotubes compared with physical absorption. The presence of polymer chains associated with SWNT will lead to a reduction of van der Waals attractions between nanotubes and will break the big ropes into small bundles. Polymer

functionalization of SWNT has many advantages over other covalent functionalization. The polymer chains will help disperse SWNT in solvents, even with a low functionalization degree, which will not change the electronic properties of SWNT much.

1) Radical Chain Polymer Attached to SWNT

Two approaches, "grafting to" and "grafting from", are employed to attach polymers to the sidewall of SWNT. "Grafting to" involves the direct reaction between the living polymer chains with the sidewalls of SWNT, which only has low density of functionalization due to the steric hindrance. However, it can produce well-controlled polymer chains prior to the grafting steps. In contrast, "grafting from" refers to growing polymer chains from the sidewall of SWNT, which has a higher functionalization degree on the surface. However, the characterization of the polymer chain cannot be obtained unless it is cleaved from the surfaces.[27, 28]

In situ free radical polymerization was the typical "grafting to" method to functionalize pristine nanotubes. The polymeric radicals generated by a thermally active reaction were added directly to the -conjugated carbon sidewall. Polyelectrolyte, such as poly(sodium 4-styrenesulfonate),[29] poly(4-vinyl pyridine) (P4VP)[30] and poly((vinylbenzyl)-trimethylammonium chloride),[31] were attached to the pristine nanotubes, and tubes were dispersed in aqueous or organic solutions.

Atom transfer radical polymerization (ATRP) is widely employed both in "grafting from" and "grafting to" method. The carboxylic acid groups were introduced by oxidation, and used to prepare ATRP macrointiator CNT-Br. Polystyrene[32, 33] was attached to sidewalls of nanotubes by both "grafting from" and "grafting to" methods. Poly(*t*-butyl acrylate),[34, 35] poly(sodium 4-styrenesulfonate),[35] polystyrene-b-poly(*t*-butyl acrylate),[33] and poly(*n*-butyl methylacrylate)[28] were "grafted from" the sidewalls of

nanotubes by ATRP. The chains attached to nanotubes were well defined, and the structure of polymers can be controlled.

2) Other Methods of Attaching Polymer to SWNT

Highly branched polymers were grafted from MWNT-OH (multi-walled carbon nanotubes) by in situ ring-opening polymerization (ROP). The reaction was carried upon cationic polymerization of 3-ethyl-3-(hydroxymethyl)oxetane (EHOX) in the presence of $BF_3 \cdot OEt_2$.[27] The nanohybrid from polymerization is polyether-functionalized nanotubes with active hydroxyl end groups. The size of the branch can be controlled by different monomer feed ratios. Ring-opening polymerization also was employed to functionalize the nanotubes with poly(*p*-dioxanone) with the tin(II) 2-ethylhexanoate as the initiator.[36]

Polymer functionalized nanotubes also were investigated by incorporation of covalent bonds between the functional groups on the sidewall with active functional groups along the polymer chains. Poly(vinyl alcohol) (PVA) was attached to nanotubes by carbodiimide-activated esterification reactions between –COOH on the sidewall of nanotubes with -OH groups of PVA.[37]

Another functionalization method that worked on fullerene was transplanted to functionalize nanotubes. Poly(N-vinylcarbazole) (PVK) and poly(1,3-butadiene) (PB) were added to the sidewalls of SWNT from a "living" anionic polymer by the introduction of polymeric carbanions generated from sodium hydride or butyllithium.[38] The Ajayan group worked on anionic polymerization of polystyrene to functionalize SWNT. First, they introduced a carbanion on the SWNT surface by sonicating pristine SWNT with *sec*-butyllithium. Then polystyrene was attached to sidewalls of SWNT with both free *sec*-butyllithium and the nanotube carbanions initiating the anionic polymerization.[39]

Characterization of Functionalized SWNT. Near infrared (NIR) and Raman spectroscopy are used to detect changes in the sidewall through chemical bond formation. Thermogravimetric analysis (TGA) indicated the weight fraction of attached groups. Atomic force microscopy (AFM) showed the changes of the size of bundles from the functionalization. ^{1}H NMR and IR were applied to confirm the functional groups attached the sidewall of nanotubes.

1. Near IR. The absorption spectrum of pristine HiPco SWNT shows van Hove singularities, which appears at 1400 nm^{-1} and 800 nm^{-1}, due to the semiconducting tubes. With the covalent functionalization which will disrupt the electronic state of SWNT, those transitions will disappear (Figure 6). Complete loss of singularities are associated with high functionalization, while in polymer functionalization, only low density polymer chains were attached to the sidewall of SWNT. Therefore, the interband transition would have less intensity, but would not disappear (Figure 7).[30, 40]

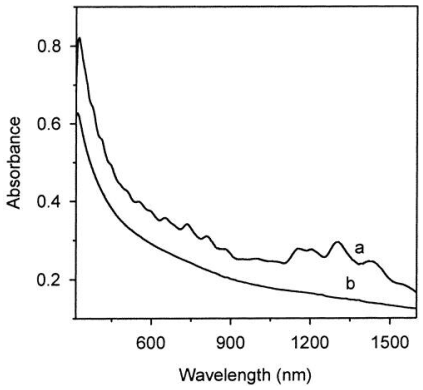

Figure 6. Absorption spectra in dimethylformamide, illustrating the loss of electronic transition structure on functionalization**;** (a) pristine SWNT, (b) aryl diazonium salts functionalized SWNT.[40]

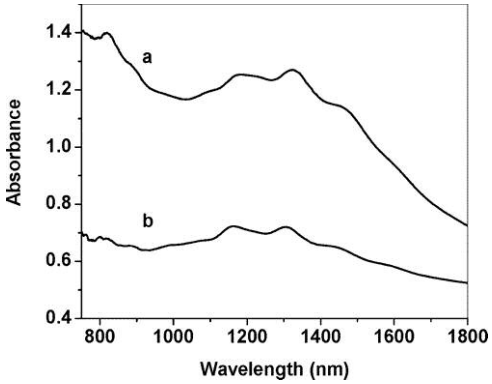

Figure 7. Transmission near-infrared spectra of films of pristine SWNT (a) and SWNT-poly(4-vinyl pyridine) (b).[30]

2. Raman. Raman spectroscopy of SWNT displays three identifying modes: One is the diameter-dependent radial breathing (ω_r) mode (RBM) between 100 cm^{-1} and 350 cm^{-1} which indicates the diameters of nanotubes, second is the higher frequency tangential (ω_t) mode (G band) between 1500 and 1600 cm^{-1}, and third is so called disorder (D band) or sp^3 hybridization between 1200 cm^{-1} and 1350 cm^{-1} which shows the character of hexagonal sidewall structure of SWNT (Figure 8). The intensity of the D band will be increased relative to the G band after covalent functionalization disrupts the sidewall structures. Therefore, it is the most important confirmatory tool of covalent functionalization of SWNT. The Raman spectra in Figure 9 show clearly that D band was increased with polymer chain attached to the SWNT.[10, 28]

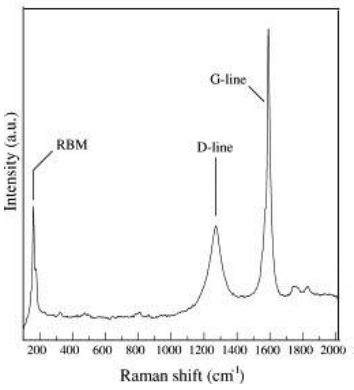

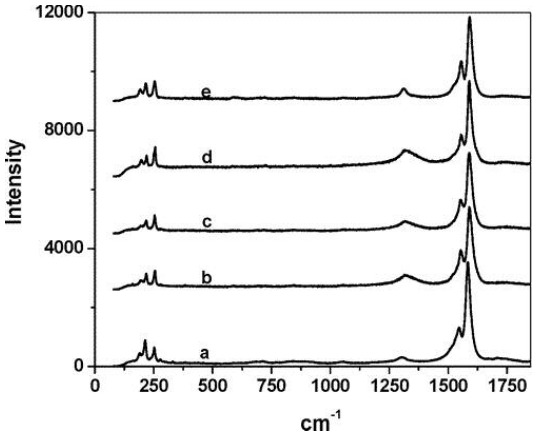

Figure 8. Raman spectrum showing the most characteristic feature of carbon nanotubes.[10]

Figure 9. Raman spectra of pristine HiPco SWNT (a), nitric acid-treated SWNT (b), SWNT-initiator (c), SWNT-g-PnBMA (d), and SWNT recovered from SWNT-g-PnBMA after TGA (e).[28]

3. TGA. Thermal gravimetric analysis gives information of the degree of functionalization after removal of the impurities and unattached polymer. The TGA from room temperature to 800 ºC under nitrogen will leave the pristine SWNT intact and decompose the polymer or other attached groups (Figure 10). The weight loss of polymers, which were attached to SWNT, shows the weight fraction of attached groups. Both the loss from carbon nanotubes from room temperature to 800 ºC and the residue, which is not volatile at 800 ºC from polymers, shall be taken into consideration.

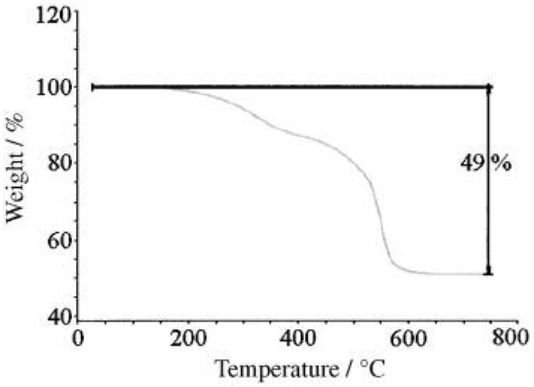

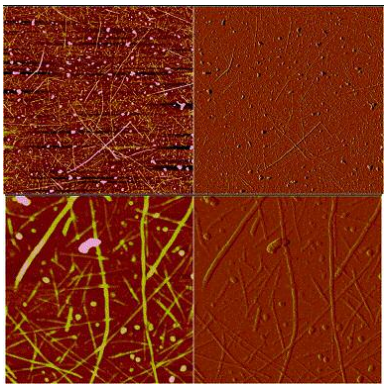

Figure 10. TGA under argon of heavily functionalized 4-chlorophenyl SWNT.[41]

Figure 11. Tapping-mode AFM images of PVP–SWNTs on a functionalized substrate. 5 μm height image (top left) and amplitude image (top right). 1μm expanded height image (bottom left) and amplitude image (bottom right).[26]

4. AFM. AFM is one of the powerful techniques in analysis of functionalization of SWNT. AFM usually is operated in tapping mode to detect the morphology. From the height image, the diameter of SWNT can be observed and compared with the diameter of individual tubes, and the consequence of functionalization can been seen (Figure 11).

Layer-by-Layer Film from Polymer-functionalized SWNT. A novel technique called "layer-by-layer" (LBL) assembly has been developed to build nanostructured systems with oppositely charged polymers and colloids since the 1990s. Layer-by-layer assembly is a general approach to prepare thin films on solid substrate from solutions. Ionic attractions (electrostatic attractions) between two opposite charged components are the driving force to prepare the film.[42]

Polyeletrolytes with a large number of ionic groups have the advantage to build the assembly because they have a large adhesion force to the solid substrate.
The assembly usually was prepared by first immersing a positively charged substrate in an anionic polyeletrolyte solution, so that a monolayer of the polyanion is absorbed on the surface. After the substrate was rinsed in pure water, it was immersed in a cationic polyeletrolyte. A monolayer of positive charge was added. By repeating the procedure in cycles, multilayer assemblies of two polymers were obtained (Figure 12).[42]

The assemblies of polyeletrolyte/carbon nanotubes were built in the same way with alternating oppositely charged polyeletrolytes and functionalized carbon nanotubes instead of two oppositely charged polyeletrolytes.

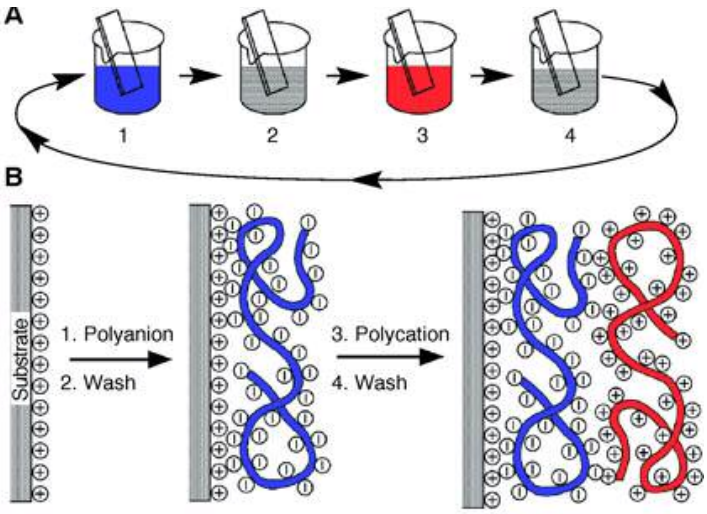

Figure 12. A) Schematic of the film deposition process using slides and beakers. Steps 1 and 3 represent the adsorption of a polyanion and polycation, respectively, and steps 2 and 4 are washing steps. (B) Simplified molecular picture of the first two adsorption steps, depicting film deposition starting with a positively charged substrate. [42]

The Kotov group published their research about construction of carbon nanotube/ polyeletrolyte multilayers in 2002. They alternated positively charged polyethylenimine (PEI) and negatively charged oxidized SWNT to prepare SWNT LBL films. The ultimate tensile strength of the films was increased to 220 ± 40 MPa after SWNT were incorporated in the assembly compared with 9 MPa of polyelectrolyte films.[43]

Kotov and coworkers recently fabricated ultra-strong layer-by-layer assembly from SWNT/polyelectrolytes.[44] The film has tensile strength close to ceramics and cermets.

Electrostatic force is employed in making the polymer/carbon nanotube multilayer films. The Rouse group reported that polycationic poly(diallyldimethylammonium chloride) (PDDA) was alternated with SWNT, which acted as polyanionic species, to form films.[45] Moreover, the Mao group did some research on the incorporation of PDDA with negatively charged mutilwalled carbon nanotubes (MWNT).[46] Qin prepared films by alternating poly(4-vinylpyridine) functionalized SWNT with poly(acrylic acid) with H bonding as the driving force between the alternating polyeletrolytes.[30]

Objective of Research

1) Because SWNT pack into bundles, they have poor solubility in organic solutions and aqueous solutions. Our objective was to obtain polymer-functionalized SWNT solutions in high concentration of nanotubes content (30~100 mg NT/L) by in situ free radical polymerization for bulk materials and LBL films.

2) Another objective was to obtain multilayer assemblies with high mechanical properties by construction of layer-by-layer (LBL) films with two opposite charged polyelectrolyte- functionalized SWNT. The multilayer assemblies can only be prepared from solutions. Consequently, the stable dispersion of SWNT in aqueous or organic solutions is required. We are interested in the improvement of tensile strength of the films after incorporation of polymer-functionalized SWNT compared with the polyelectrolyte films. We expected thatthe tensile strength of our LBL films of 40 bilayers would exceed 220 MPa, which is reported from SWNT/ polymer binary systems that Kotov's group prepared.[43]

CHAPTER II

EXPERIMENTAL

Materials. *tert*-Butyl acrylate (Aldrich, 98%) and styrene (Acros, 99%) were purified by passing through basic alumina before use. Sodium acrylate (Aldrich, 97%) was used as received. Azobis(isobutyronitrile) (AIBN) and potassium persulfate (KPS) were used as received from Aldrich, and N,N-dimethylformamide (DMF) was used as received from Pharmco. Poly(diallyldimethylammonium chloride) (PDDA) (Aldrich, 20%, M_w = 400 000~ 450 000) was diluted to 1% before use. Single-walled carbon nanotubes were purchased from Carbon Nanotechologies Inc., Houston TX (HiPco, batch no: PO175).

Instruments and Measurements. Atomic force micrographs (AFM) were obtained using a Multimode Nanoscope IIIa SPM (Digital Instruments, St. Barbara, CA) operating in the tapping mode. The samples for AFM measurements were prepared by evaporating several drops of dilute solutions of functionalized SWNT on a mica surface. TGA data was obtained using 3~5 mg samples with a Shimadzu TGA50/50H thermogravimetric analyzer in a nitrogen atmosphere. Infrared (IR) spectra were recorded on a Perkin-Elmer 2000 FTIR instrument. The IR samples were prepared by evaporating polymer-functionalized solutions on CaF_2 windows to form thin films. The Raman samples were prepared by evaporating solution on silicon wafers to form thin

films. Raman measurements were then carried out on a Jobin Yvon microRaman system (Ramanor U1000, Instruments SA, USA) using a Spectra-Physics Ar ion laser at an excitation wavelength of 514.5 nm (2.41 eV).

Polymer/Copolymer Functionalized SWNT in DMF. A 50 mL dried Schlenk flask was charged with a magnetic stirrer, 60 mg of pristine SWNT, and 30 mL of DMF. After stirring for 12 h at room temperature, AIBN (2 mol% of monomer) and 6.0 g of monomer were added. The solution was stirred for 15 min at 0 °C. The mixture was degassed by three freeze-pump-thaw cycles. The flask was placed in a thermostated oil bath at 65 ˚C for 48 h with stirring. After polymerization, the mixture was diluted to 200 mL with fresh DMF and was centrifuged at 5,000 ×g for 2 h. The yellowish supernatant polymer solution was decanted. The black precipitate was redispersed in DMF by shaking, and centrifugation and decantation were repeated once. We used gentle centrifugation and decantation cycles to remove the supernatant polymer solutions and reduce the content of free polymers. Otherwise, the following ultrafiltration process will proceed very slowly because the high content polymer together with nanotubes will clog the membrane pores. The free polymer was collected by evaporation of solvent from the supernatant solutions and dried in a vacuum oven at 50 ºC prior to TGA and IR analysis.

The sediments were diluted to 200 mL with fresh DMF, bath-sonicated for 1 h, and gently centrifuged at 5,000 ×g for 3 h. Bath sonication was applied to de-bundle the SWNT ropes and to make a black solution. After removal of the supernatant black solution, the sediments were redispersed in DMF by bath-sonication for 10 min, and the mixture was centrifuged at 5,000 ×g for 3 h. The supernatant was collected, and the procedure was repeated two more times.

The combined black supernatant solution was vacuum-filtered through a 0.2 μm PTFE membrane. After washing eight times with 40 mL of DMF each time, no cloudiness appeared when ten drops of filtrate was added to 15 mL of non-solvents of polymers, indicating that little or no soluble free polymer remained in the mixture. A black solid was collected on the membrane, and was dried in vacuum for 36 h at 50 °C. The details of reactions are shown in Table 1. The scheme of experimental procedure was shown in Appendix 1.

Table 1. Conditions of Polymerization in DMF

	PS-SWNT	PtBA-SWNT	(PS-co-PtBA)-SWNT
monomer	styrene, 6 g	tBA, 6 g	styrene, 4 g tBA, 2 g
initiator	AIBN, 190 mg	AIBN, 160 mg	AIBN, 180 mg
non-solvents for polymers	methanol	concentrated HCl/methanol (1:10 v/v)	methanol
sample numbers	2-77	2-76, 2-90	2-94, 2-95

Poly(sodium acrylate) Functionalized SWNT in Water. A 30 mL round bottomed flask was charged with a magnetic stirrer, 30 mg of pristine SWNT, and 15 mL of DMF. After stirring for 24 h, the mixture was centrifuged at 5000 ×g, and the supernatant colorless liquid was decanted. The black sediments were washed with

methanol and deionized water three times each. The same centrifugation-decantation-wash cycle was repeated three times. Then SWNT were transferred to a dried Schlenk flask, which was charged with a magnetic stirrer, 30 mL of deionized water, KPS (2.5 mol% of monomer), and 4.0 g of sodium acrylate. The mixture was stirred 15 min at 0 °C and degassed by three freeze-pump-thaw cycles. The flask was placed in a thermostated oil bath at 65 ˚C for 48 h with stirring. After polymerization, the mixture was diluted to 200 mL with fresh deionized water and centrifuged at 5,000 ×g for 2 h. The yellowish supernatant polymer solution was decanted. The black precipitate was redispersed in deionized water by shaking, and centrifugation and decantation were repeated once. The free polymer was collected by evaporation of solvent from the supernatant solutions and was dried in a vacuum oven at 50 ºC prior to TGA and IR analysis.

The sediments were diluted to 200 mL with fresh deionized water, bath-sonicated for 1 h, and gently centrifuged at 5,000 ×g for 3 h. After removal of the supernatant black solution, the sediments were redispersed in deionized water by bath sonication for 10 min. After the dispersion was centrifuged at 5,000 ×g for 3 h, the supernatant was collected, and the solid was washed and centrifuged two more times.

The combined supernatant black solution was vacuum-filtered through a 0.2 μm PTFE membrane. After washing eight times with 40 mL of deionized water, no cloudiness appeared when ten drops of filtrate was added to 15 mL of absolute ethanol, indicating that little or no soluble free polymer remained in the mixture. A black solid was collected on the membrane and was dried in vacuum for 36 h at 50 °C. Samples from three separate preparations were numbered as 2-54, 2-93, and 2-96.

PAA Functionalized SWNT from Deprotection of PtBA-SWNT or (PS-co-PtBA)-SWNT. PtBA-SWNT or (PS-co-PtBA)-SWNT (10 mg) was stirred magnetically in 5 mL of CH_2Cl_2 at room temperature for 24 h. Then 1 mL of trifluoroacetic acid (TFA) was added dropwise, and the mixture was stirred another 12 h at room temperature. The solvent and excess TFA were evaporated by gentle N_2 bubbling. Black solid was collected.

PAA Funtionalized SWNT from Acidification of PNaA-SWNT. An HCl solution 20 mL (pH = 2.1) was added to a 20 mL solution of PNaA-SWNT dropwise. The black aggregates form immediately. Excess HCl was removed by centrifugation-decantation-wash cycles as described in the section on poly(sodium acrylate) functionalized SWNT in water.

(PNaA-SWNT/PVBTMACl-SWNT)$_n$ Multilayer Films. Poly(vinylbenzyl)-trimethylammonium chloride) functionalized SWNT (PVBTMACl-SWNT) was prepared by Maxim Tchoul.[31] A 3×1 cm^2 glass slide was cleaned in 50 mM NaOH by bath sonication 15 min and rinsed three times with water. The glass was immersed in an aqueous poly(diallyldimethylammonium chloride) (PDDA) (1 %) solution for 1 h and was rinsed by dipping in fresh water for 1 min three times. Bilayers of (PNaA-SWNT/ PVBTMACl-SWNT) were coated by alternately dipping into a 30 mg NT/L PNaA-SWNT solution for 1 h. The sample was rinsed with water three times, dipped into a 30 mg NT/L PVBTMACl-SWNT solution for 1 h, and rinsed with water three times.

CHAPTER III

RESULTS AND DISCUSSION

Polystyrene-functionalized SWNT. PS-SWNT was prepared by grafting polymer to sidewall of SWNT through in situ free radical polymerization in DMF. Black solid was collected after bath-sonication, gentle centrifugation, and ultrafiltration. The sample numbered 2-77 was used in the characterization.

The FTIR spectra of PS-SWNT show peaks at 3021 cm^{-1} and 1601 cm^{-1}, which are assigned to the aromatic rings of polystyrene (see Appendix 2). The AFM image in Figure 1 shows the heights of tubes vary from 1.1 to 1.8 nm and average 1.6 nm from ten measurements of different segments of tubes in the image. The diameter of bundles of pristine HiPco SWNT is in the order of 10 nm.[47] Therefore, the big bundles were broken into small ones by polymer functionalization. We conjecture that the white spots in the image might be free polymer particles.

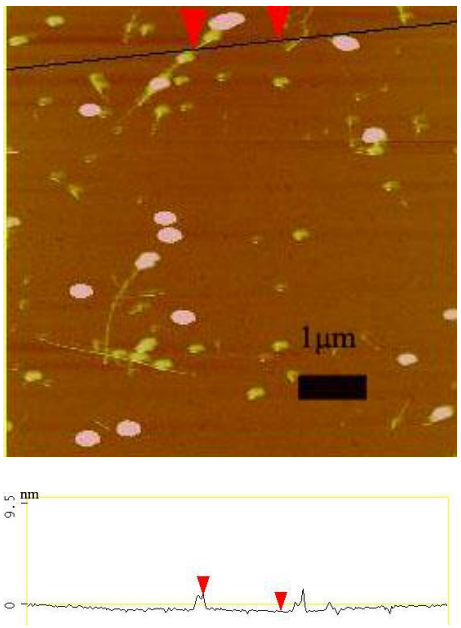

Figure 1. AFM height image of PS-SWNT

TGA of the SWNT-PS indicated a 28% weight loss in a nitrogen atmosphere at 800 °C (Figure 2). SWNT gave 7% weight loss at 800 ºC, and the polymer was decomposed from 400 °C and gave 2% residue which was not volatile at 800 °C. We assume that the polymer-SWNT composites contain x% of nanotubes and y% of polymers. We can use the equations as below to calculate the polymer content of composites.

$$x\% + y\% = 100\%$$
$$7\% \times x\% + (1 - 2\%) \times y\% = 28\%$$

Therefore, y%=23%. From the calculation, the composites contain 23% of PS.

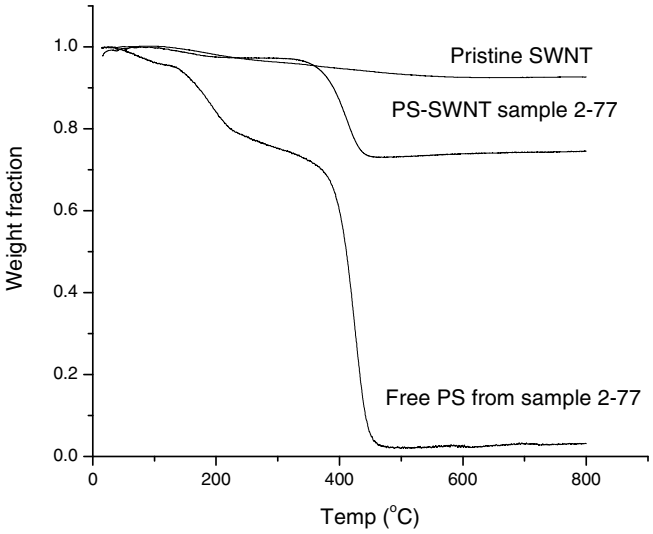

Figure 2. TGA thermograms of pristine SWNT, PS SWNT, and PS

Raman spectra indicate the sidewall functionalization. The disorder mode at 1345 cm^{-1}shows sp^3 character of the sidewall of SWNT. The intensity of the disorder mode was increased with respect to the G band at 1500~1600 cm^{-1} after polymer functionalization, which indicates that the covalent bond between the SWNT and the polymer chains changes the sp^2 hybridization of a significant number of carbon atoms of the nanotubes to sp^3 hybridization (Figure 3).

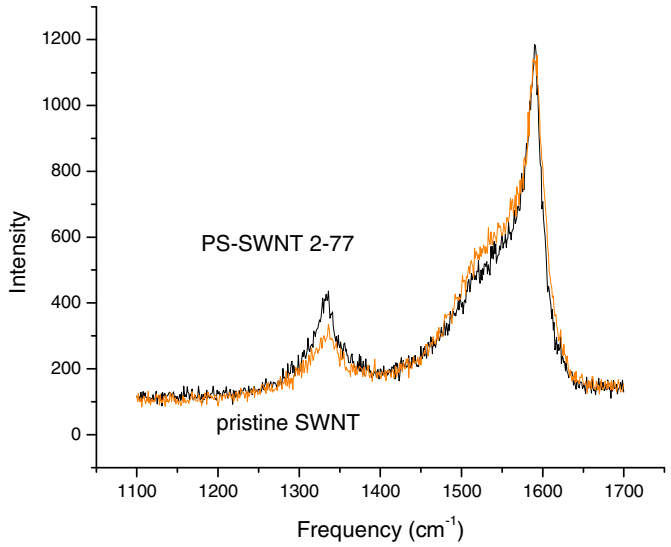

Figure 3. Raman spectra of pristine SWNT and PS-SWNT

PS-SWNT is one of first samples we successfully prepared in DMF solutions. We determined that the initiator/ monomer ratio should be ~ 2%. Lower initiator/monomer did not lead to well-dispersed polymer functionalized SWNT samples, which might be due to carbon nanotubes with π sidewall frameworks functioning as inhibitors in the reactions. It was decided to choose DMF asthe solvent for polymerizations, instead of*o* -dichlorobenzene (O-DCB). O-DCB is a good solvent itself for carbon nanotubes by forming sonopolymers which wrap to the nanotubes. HiPco SWNT dispersed in O-DCB, after strong sonication, showed a marked increase in the D-band intensity with respect to the G band intensity.[48]

Qin[32] and Kong[33] employed atom transfer radical polymerization (ATRP) to functionalize carbon nanotubes with PS, in which a well-defined polymer was attached to nanotubes and a higher weight loss (85%) was achieved. Although we only achieved 23% weight loss from PS decomposition, we obtained stable dispersed solutions.

Moreover, the in situ free radial polymerization we used is a facile method compared with ATRP which involves strict reaction conditions and a multi-step process

Poly(tert-butyl actylate)-functionalized SWNT. PtBA-SWNT was prepared by grafting polymer to the sidewall of SWNT through an in situ free radical polymerization. Black solid was collected after bath-sonication, gentle centrifugation, and ultrafiltration. The sample numbered 2-76 was used in characterization.

The FTIR spectra of PtBA-SWNT composites show a new strong peak at 1723 cm^{-1} due to carbonyl absorption of PtBA compared with pristine SWNT (see Appendix 3). The AFM image in Figure 4 shows that the heights of tubes vary from 3.0 to 10.3 nm and average 6.5 nm from fourteen measurements of different segments of tubes in the image. The image indicates that the big bundles of pristine tubes were broken into some small diameter nanotube bundles by polymer functionalization. The image was taken right after 30 min of bath sonication of solutions, and the white spots all over the image might be amorphous carbon from nanotubes damaged from sonication. TGA of the SWNT-PtBA gave a 30% weight loss in a nitrogen atmosphere at 800 °C (Figure 5). The polymer was decomposed from 280 °C and gave a 10% residue which was not volatile at 800 °C, which indicates that the composite contained 28% PtBA from the calculation of the weight loss from pristine SWNT and PtBA (calculation described in polystyrene-functionalized SWNT section). Raman spectra show that disorder mode at 1345 cm^{-1} of functionalized SWNT was enhanced with respect to the G band intensity after polymer

functionalization, which supports the covalent functionalization of sidewalls of nanotubes (Figure 6).

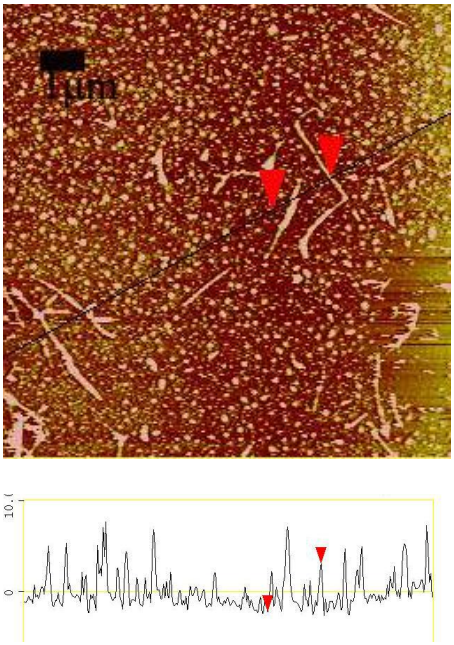

Figure 4. AFM height image of PtBA-SWNT

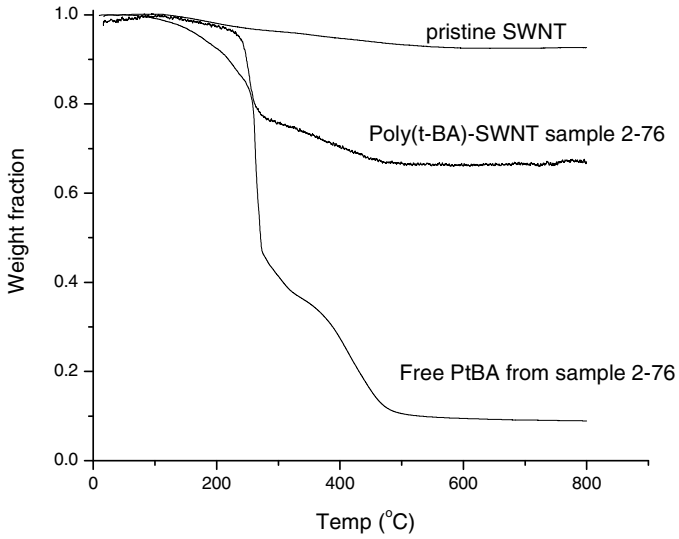

Figure 5. TGA thermograms of pristine SWNT, PtBA-SWNT, and PtBA

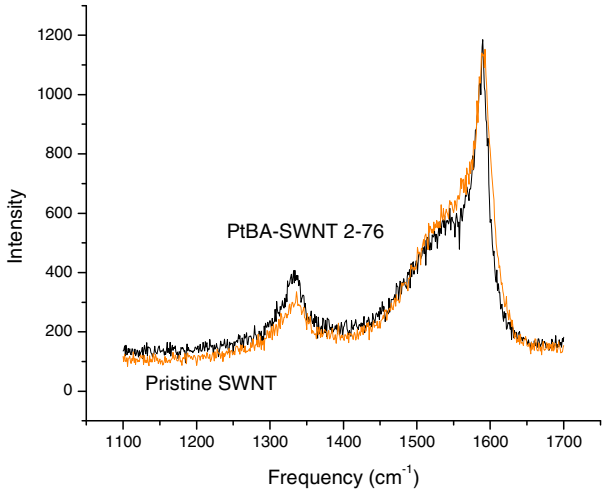

Figure 6. Raman spectra of pristine SWNT and PtBA-SWNT

PtBA-SWNT also is one of the first samples successfully prepared in DMF. We could not prepare stable dispersed PAA-SWNT from deprotection of PtBA-SWNT , and only found black precipitate in aqueous solutions. Yao[34] and Kong[35] employed living polymerization to attach PtBA to the carbon nanotubes. They obtained well dispersed PAA-SWNT solutions from deprotection of *t*-butyl group. However, they did not provide any information about polymer content in the composites and polymer chain morphology. Therefore, we could not compare our PAA-SWNT with their samples..

Poly(styrene co-tert-butyl acrylate)-functionalized SWNT. (PS-co-PtBA)-SWNT was prepared from mixed styrene and tBA monomers through an in situ free radical copolymerization. Black solid was collected after bath-sonication, gentle centrifugation, and ultrafiltration. The sample numbered 2-94 was used in characterization.

FTIR spectra of copolymer functionalized SWNT show a new peak at 1729 cm^{-1} due to the carbonyl vibration of PtBA compared with pristine SWNT (see Appendix 4). A ^{1}H NMR spectrum of the free polymer was not resolved sufficiently to calculate the copolymer composition from the peak areas. The AFM image in Figure 7 shows that the heights of tubes vary from 1.0 nm to 10.8 nm and average 4.8 nm from fifteen measurements of different segments of tubes in the image. The image indicates that the large bundles of pristine tubes were broken into some small diameter nanotube bundles by polymer functionalization. TGA of copolymer functionalized SWNT shows a 37% weight loss in a nitrogen atmosphere at 800 °C (Figure 8), and the curve also shows two decomposition slopes around 280 °C and 400 °C which match observation with TGA curves of PS and PtBA. TGA analysis indicates copolymer-SWNT composites contain 33% attached polymers (calculation described in polystyrene-functionalized SWNT section). Raman spectra indicate the intensity of disorder mode at 1345 cm^{-1} was increased relative to the G band after polymer functionalization, which indicates there are covalent bonds between the SWNT and polymer chains (Figure 9).

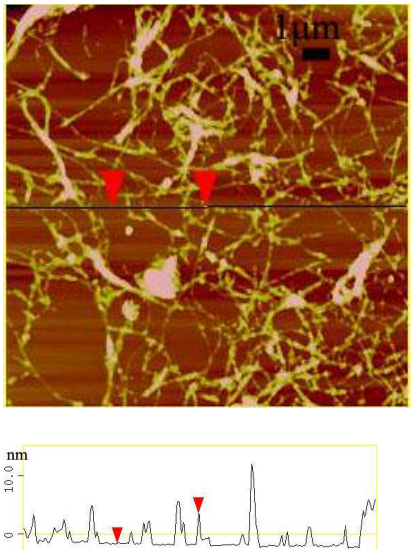

Figure 7. AFM height image of (PS-co-PtBA)- SWNT

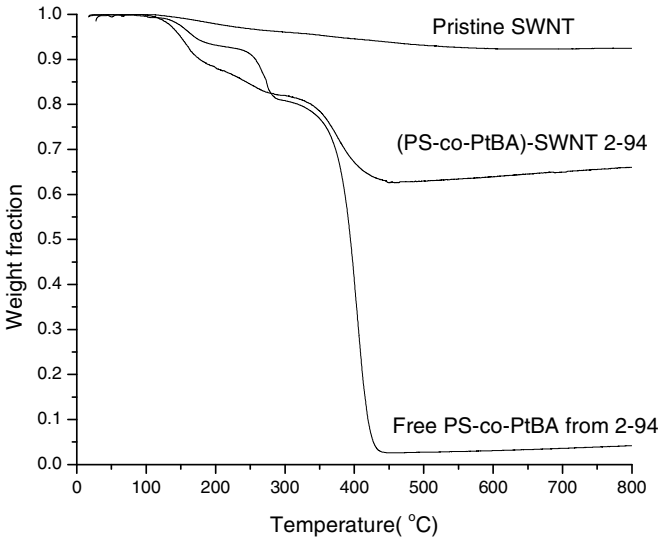

Figure 8. TGA thermograms of pristine SWNT, (PS-co-PtBA)-SWNT, and PS-co-PtBA (The slight increase of curves after 450 ºC is due to an instrumental calibration problem.)

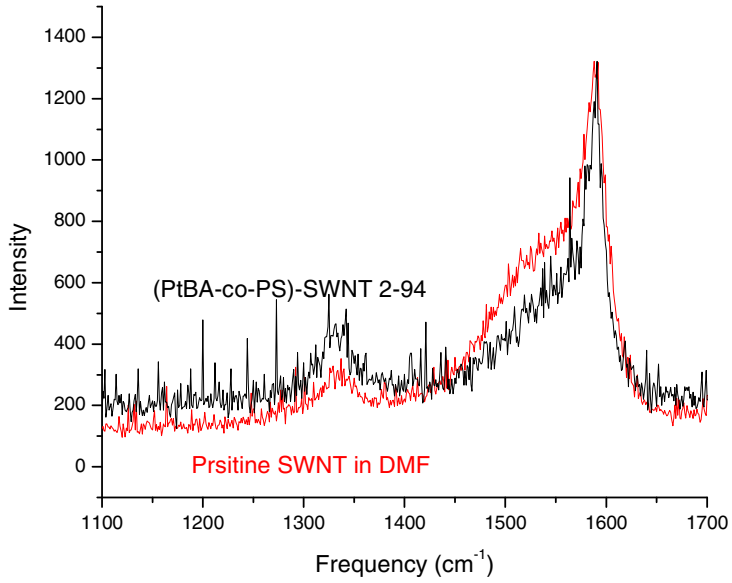

Figure 9. Raman spectra of (PS-co-PtBA)- SWNT and pristine SWNT

After deprotetction, we prepared (PS-co-PAA)-SWNT. Several solvent mixtures were used to dissolve the composites, but only black solid precipitate was found in those solvents. Adronov's group[49] used nitroxide-mediated "living" free-radical

polymerization to prepare (PS-b-PtBA)-functionalized carbon nanotubes. The weight loss of their nanotube composites is 62%, while we only have 33% weight loss of attached polymer. After deprotection, they[49] found PAA-b-PS soluble in mixture of chloroform and methanol of various compositions. This different solubility of their samples and ours in organic solvents might be due to the difference in polymer morphology from a random copolymer and a block copolymer.

Poly(sodium acrylate)-functionalized SWNT. PNaA-SWNT was prepared by grafting polymer to the sidewalls of SWNT through an in situ free radical polymerization in water. Black solid was collected after bath-sonication, gentle centrifugation, and ultrafiltration. The sample numbered 2-93 is used in characterization.

The AFM image in Figure 10 shows that the heights of tubes vary from 4.9 nm to 8.6 nm and average 6.3 nm from eleven measurements of different segments of tubes in the image. TGA of PNaA-SWNT showed a 77% weight loss in a nitrogen atmosphere at 700 °C (Figure 11), indicating that the PNaA-SWNT composites contain 53% attached polymer (calculation described in polystyrene-functionalized SWNT section).

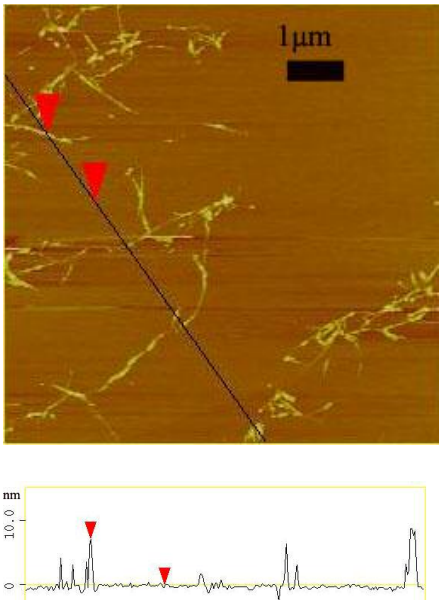

Figure 10. AFM heightimage of PNaA -SWNT

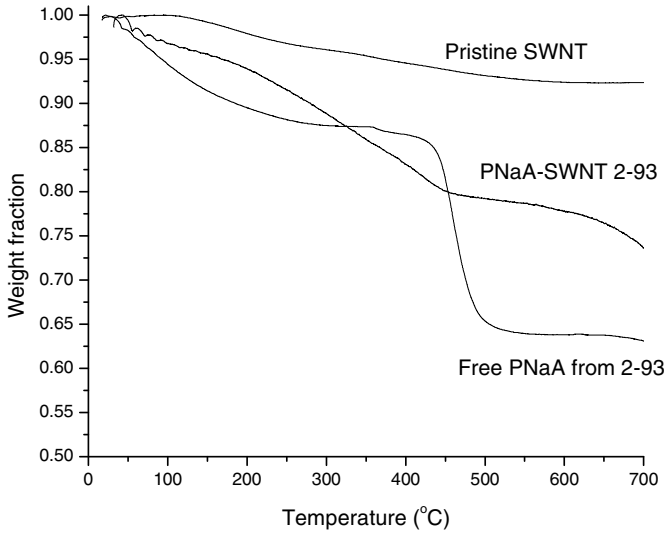

Figure 11. TGA thermograms of pristine SWNT, PNaA-SWNT, and PNaA

Raman spectra show the intensity of the disorder mode at 1345 cm^{-1} was increased relative to the G band after polymer functionalization, which indicates covalent bonding between the SWNT and polymer chains (Figure 12).

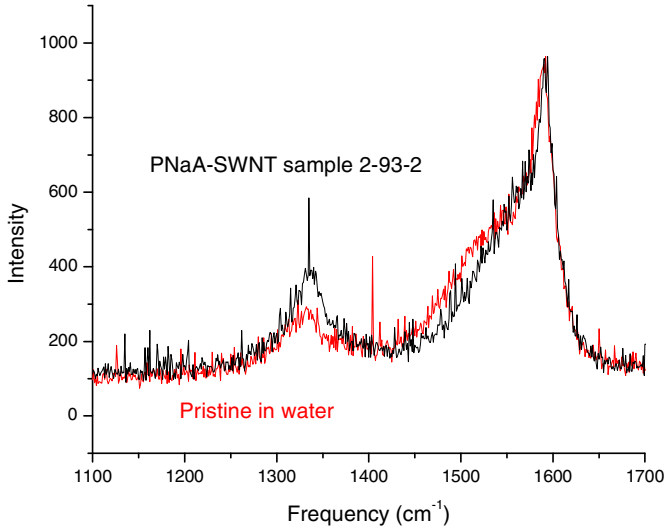

Figure 12. Raman spectra of PNaA-SWNT and pristine SWNT

We functionalized carbon nanotubes by an in situ free radical polymerization of sodium acrylate. Instead of deprotection from *t*-butyl group,[34, 35] we attached negatively charged poly(sodium acrylate) to the sidewall of SWNT directly, which is a one step reaction without heavy sonication. This process gave a stable black solution which can be used in fabrication of LBL films.

Dispersion of Polymer-functionalized SWNT. Pristine SWNT precipitated in DMF or water solutions (Figure 13a). Pristine SWNT also precipitated in a mixture of monomer/DMF before polymerization. Stable dispersions as homogeneous black solutions were obtained from PS-SWNT in DMF, PtBA-SWNT in DMF, (PS-co-PtBA)-SWNT in DMF, and PNaA-SWNT in water (Figure 13b~e). PAA-SWNT samples were prepared by deprotection or acidification of the above well dispersed samples, but none of the PAA-SWNT samples were dispersed well in water, methanol, or mixed organic solvents (Figure 13f~h).

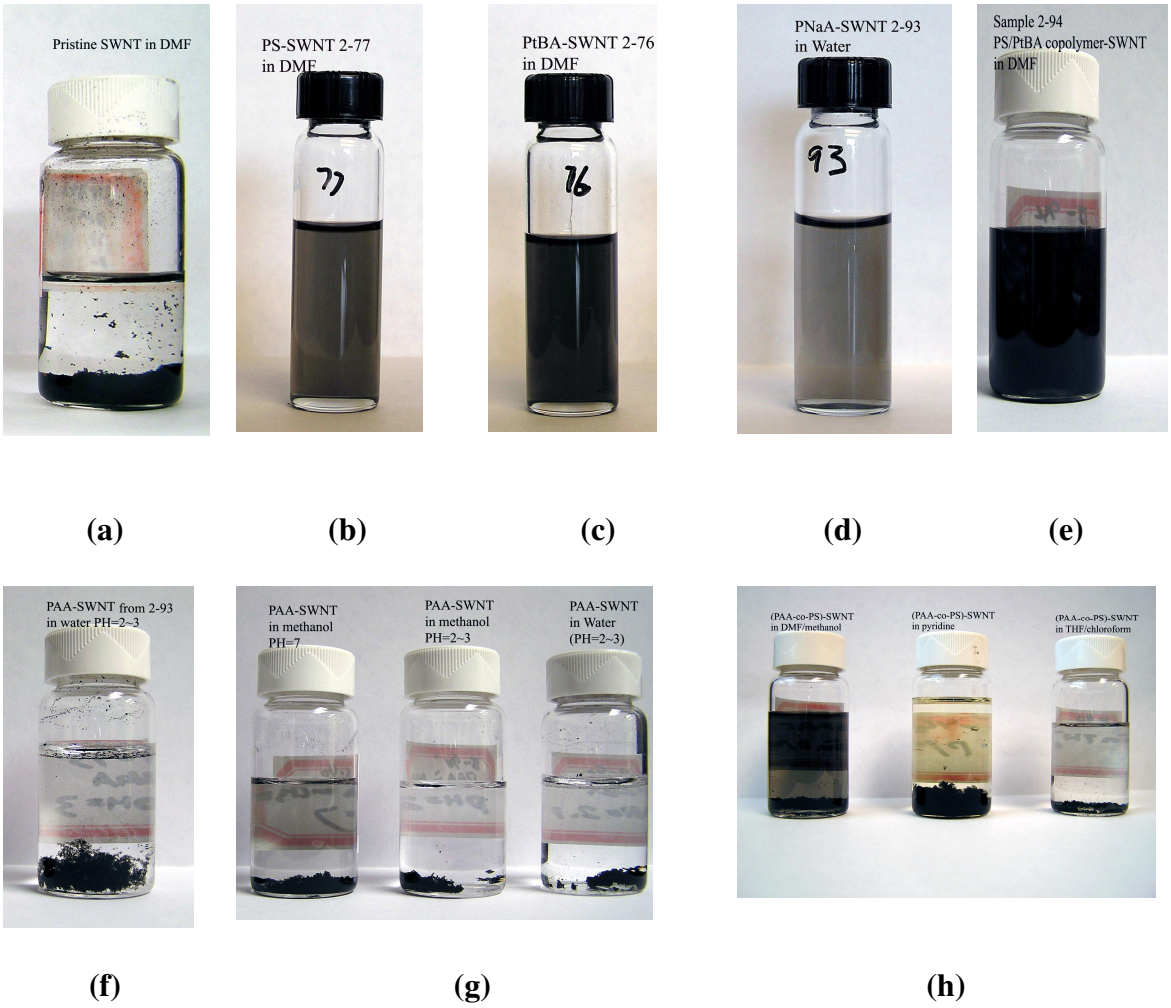

Figure 13. Dispersion of polymer functionalized SWNT samples after two weeks: a) pristine in DMF, b) PS-SWNT in DMF, c) PtBA-SWNT in DMF, d) PNaA-SWNT in water, e) (PS-co-PtBA)-SWNT, f) PAA-SWNT (acidification from PNaA-SWNT), g) PAA-SWNT (deprotection from PtBA-SWNT), h) (PAA-co-PS)-SWNT (deprotection from (PtBA-co-PS)-SWNT))

UV-vis Absorption of Multilayer Films of Polyelectrolyte Functionalized SWNT. The layer by layer films were prepared by alternating PNaA-SWNT with PVBTMACl-SWNT. Figure 14 shows the UV-vis absorption spectra of polyelectrolyte functionalized SWNT multilayer films with different numbers of bilayers. We use air as the reference for the spectra, so that the absorbance comes from both glass and the bilayers. Although thespectra are noisy, the linear increase of absorbance at 400 nm with numbers of bilayers indicates uniform thickness of deposited bilayers. The insert in Figure 14 shows absorbance at 400 nm vs. number of bilayers using absorbance values from averaging of spectra noise.

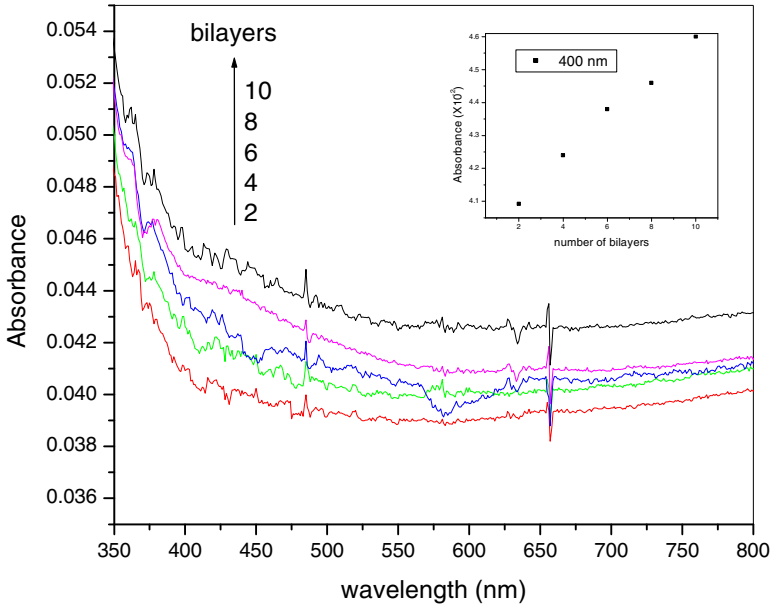

Figure 14. UV-vis absorption spectra of PNaA-SWNT/ PVBTMACl-SWNT multilayer films with different numbers of bilayers.

CHAPTER IV

CONCLUSIONS

Stable dispersions of PS-SWNT in DMF, PtBA-SWNT in DMF, (PS-co-PtBA)-SWNT in DMF, and PNaA-SWNT in water were obtained by in situ free radical polymerization. AFM images show big bundles were broken into small ones after functionalization, and Raman spectra indicate covalent functionalization of sidewalls of SWNT from increase of D-band intensity with respect to G-band intensity.

LBL films from two oppositely charged polyelectrolyte functionalized SWNT will be prepared in the laboratory of Nicholas Kotov at the University of Michigan. With high content of SWNT incorporated into the films, we expect the tensile strength of 40 bilayer films will exceed 220 MPa.

REFERENCES

(1) Iijima, S. *Nature* **1991,** 354, 56-58.

(2) Iijima, S. *Physica B* **2002,** 323, 1-5.

(3) Bethune, D. S.; Kiang, C. H.; de Vries, M. S.; Gorman, G.; Savoy, R.; Vazquez, J.; Beyers, R. *Nature* **1993,** 363, 605-7.

(4) Iijima, S.; Ichihashi, T. *Nature* **1993,** 364, 737.

(5) Ajayan, P. M. *Chem. Rev.* **1999,** 99, 1787-1799.

(6) Terrones, M. *Int. Mater. Rev.* **2004,** 49, 325-377.

(7) Dresselhaus, M. S.; Dresselhaus, G.; Avouris, P.*Carbon Nanotubes Synthesis, Structure, Properties, and Applications;* Springer: Berlin, 2001.

(8) Nikolaev, P.; Bronikowski, M. J.; Bradley, R. K.; Rohmund, F.; Colbert, D. T.; Smith, K. A.; Smalley, R. E. *Chem. Phys. Lett.* **1999,** 313, 91-97.

(9) Kitiyanan, B.; Alvarez, W. E.; Harwell, J. H.; Resasco, D. E. *Chem. Phys. Lett.* **2000,** 317, 497.

(10) Belin, T.; Epron, F. *Mater. Sci. Eng. B* **2005,** 119, 105-118.

(11) Biercuk, M. J.; Llaguno, M. C.; Radosavljevic, M.; Hyun, J. K.; Johnson, A. T.; Fischer, J. E. *App. Phsy. Lett.* **2002,** 80, 2767-2769.

(12) Bianco, A.; Kostarelos, K.; Partidos, C. D.; Prato, M. *Chem. Commun.* **2005**, 571-577.

(13) Nagasawa, S.; Yudasaka, M.; Hirahara, K.; Ichihashi, T.; Iijima, S. *Chem. Phys.*

Lett. **2000,** 328, 374-380.

(14) Gajewski, S.; Maneck, H. E.; Knoll, U.; Neubert, D.; Dorfel, I.; Mach, R.; Strauss, B.; Friedrich, J. F. *Diamond Relat. Mater.* **2003,** 12, 816-820.

(15) Chen, J.; Rao, A. M.; Lyuksyutov, S.; Itkis, M. E.; Hamon, M. A.; Hu, H.; Cohn, R. W.; Eklund, P. C.; Colbert, D. T.; Smalley, R. E.; Haddon, R. C. *J. Phys. Chem. B* **2001,** 105, 2525-2528.

(16) Liu, J.; Rinzler, A. G.; Dai, H. J.; Hafner, J. H.; Bradley, R. K.; Boul, P. J.; Lu, A.; Iverson, T.; Shelimov, K.; Huffman, C. B.; Rodriguez-Macias, F.; Shon, Y. S.; Lee, T. R.; Colbert, D. T.; Smalley, R. E. *Science* **1998,** 280, 1253-1256.

(17) Ziegler, K. J.; Gu, Z.; Peng, H.; Flor, E. L.; Hauge, R. H.; Smalley, R. E. *J. Am. Chem. Soc.* **2005,** 127, 1541-1547.

(18) Vazquez, E.; Georgakilas, V.; Prato, M. *Chem. Commun.* **2002**, 2308-2309.

(19) Mickelson, E. T.; Huffman, C. B.; Rinzler, A. G.; Smalley, R. E.; Hauge, R. H.; Margrave, J. L. *Chem. Phys. Lett.* **1998,** 296, 188-194.

(20) Khabashesku, V. N.; Billups, W. E.; Margrave, J. L. *Acc. Chem. Res.* **2002,** 35, 1087-1095.

(21) Dyke, C. A.; Tour, J. M. *Nano Lett.* **2003,** 3, 1215-1218.

(22) Liang, F.; Sadana, A. K.; Peera, A.; Chattopadhyay, J.; Gu, Z. N.; Hauge, R. H.; Billups, W. E. *Nano Lett.* **2004,** 4, 1257-1260.

(23) Georgakilas, V.; Kordatos, K.; Prato, M.; Guldi, D. M.; Holzinger, M.; Hirsch, A. *J. Am. Chem. Soc.* **2002,** 124, 760-761.

(24) Holzinger, M.; Abraham, J.; Whelan, P.; Graupner, R.; Ley, L.; Hennrich, F.; Kappes, M.; Hirsch, A. *J. Am. Chem. Soc.* **2003,** 125, 8566-8580.

(25) Coleman, K. S.; Bailey, S. R.; Fogden, S.; Green, M. L. H. *J. Am. Chem. Soc.* **2003,** 125, 8722-8723.

(26) O'Connell, M. J.; Boul, P.; Ericson, L. M.; Huffman, C.; Wang, Y. H.; Haroz, E.; Kuper, C.; Tour, J.; Ausman, K. D.; Smalley, R. E. *Chem. Phys. Lett.* **2001,** 342, 265-271.

(27) Xu, Y. Y.; Gao, C.; Kong, H.; Yan, D. Y.; Jin, Y. Z.; Watts, P. C. P. *Macromolecules* **2004,** 37, 8846-8853.

(28) Qin, S. H.; Oin, D. Q.; Ford, W. T.; Resasco, D. E.; Herrera, J. E. *J. Am. Chem. Soc.* **2004,** 126, 170-176.

(29) Qin, S. H.; Qin, D. Q.; Ford, W. T.; Herrera, J. E.; Resasco, D. E.; Bachilo, S. M.; Weisman, R. B. *Macromolecules* **2004,** 37, 3965-3967.

(30) Qin, S. H.; Qin, D. Q.; Ford, W. T.; Herrera, J. E.; Resasco, D. E. *Macromolecules* **2004,** 37, 9963-9967.

(31) Tchoul, M. N.; Ford, W. T.; Gheith, M. K.; Wicksted, J. P.; Motamedi, M. *Polym. Prepr. (Am. Chem. Soc., Div. Polym. Chem.)* **2005,** 46, 222-223.

(32) Qin, S. H.; Qin, D. Q.; Ford, W. T.; Resasco, D. E.; Herrera, J. E. *Macromolecules* **2004,** 37, 752-757.

(33) Kong, H.; Gao, C.; Yan, D. Y. *Macromolecules* **2004,** 37, 4022-4030.

(34) Yao, Z. L.; Braidy, N.; Botton, G. A.; Alex, A. T. *J. Am. Chem. Soc.* **2003,** 125, 16015-16024.

(35) Kong, H.; Luo, P.; Gao, C.; Yan, D. *Polymer* **2005,** 46, 2472-2485.

(36) Yoon, K. R.; Kim, W. J.; Choi, I. S. *Macromol. Chem. Phys.* **2004,** 205, 1218-1221.

(37) Lin, Y.; Zhou, B.; Fernando, K. A. S.; Liu, P.; Allard, L. F.; Sun, Y. P. *Macromolecules* **2003,** 36, 7199-7204.

(38) Wu, W.; Zhang, S.; Li, Y.; Li, J. X.; Liu, L. Q.; Qin, Y. J.; Guo, Z. X.; Dai, L. M.; Ye, C.; Zhu, D. B. *Macromolecules* **2003,** 36, 6286-6288.

(39) Viswanathan, G.; Chakrapani, N.; Yang, H.; Wei, B.; Chung, H.; Cho, K.; Ryu, C. Y.; Ajayan, P. M. *J. Am. Chem. Soc.* **2003,** 125, 9258-9259.

(40) Bahr, J. L.; Yang, J. P.; Kosynkin, D. V.; Bronikowski, M. J.; Smalley, R. E.; Tour, J. M. *J. Am. Chem. Soc.* **2001,** 123, 6536-6542.

(41) Dyke, C. A.; Tour, J. M. *Chem--Eur.J.* **2004,** 10, 813-817.

(42) Decher, G. *Science* **1997,** 277, 1232-1237.

(43) Mamedov, A. A.; Kotov, N. A.; Prato, M.; Guldi, D. M.; Wicksted, J. P.; Hirsch, A. *Nature Mater.* **2002,** 1, 190-194.

(44) Kotov, N. A.; Mamedov, A. A.; Guldi, D. M.; Prato, M.; Wicksted, J.; Hirsch, A. *PMSE Preprints* **2004,** 90, 325.

(45) Rouse, J. H.; Lillehei, P. T. *Nano Lett.* **2003,** 3, 59-62.

(46) Zhang, M. N.; Yan, Y. M.; Gong, K. P.; Mao, L. Q.; Guo, Z. X.; Chen, Y. *Langmuir* **2004,** 20, 8781-8785.

(47) Izard, N.; Riehl, D.; Anglaret, E. *Phys. Rev. B: Condens. Matter Mater. Phys.* **2005,** 71, 195417/1-195417/7.

(48) Niyogi, S.; Hamon, M. A.; Perea, D. E.; Kang, C. B.; Zhao, B.; Pal, S. K.; Wyant, A. E.; Itkis, M. E.; Haddon, R. C. *J. Phys. Chem. B* **2003,** 107, 8799-8804.

(49) Liu, Y.; Yao, Z.; Adronov, A. *Macromolecules* **2005,** 38, 1172-1179.

APPENDICES

Appendix 1. Scheme of Experimental Procedure

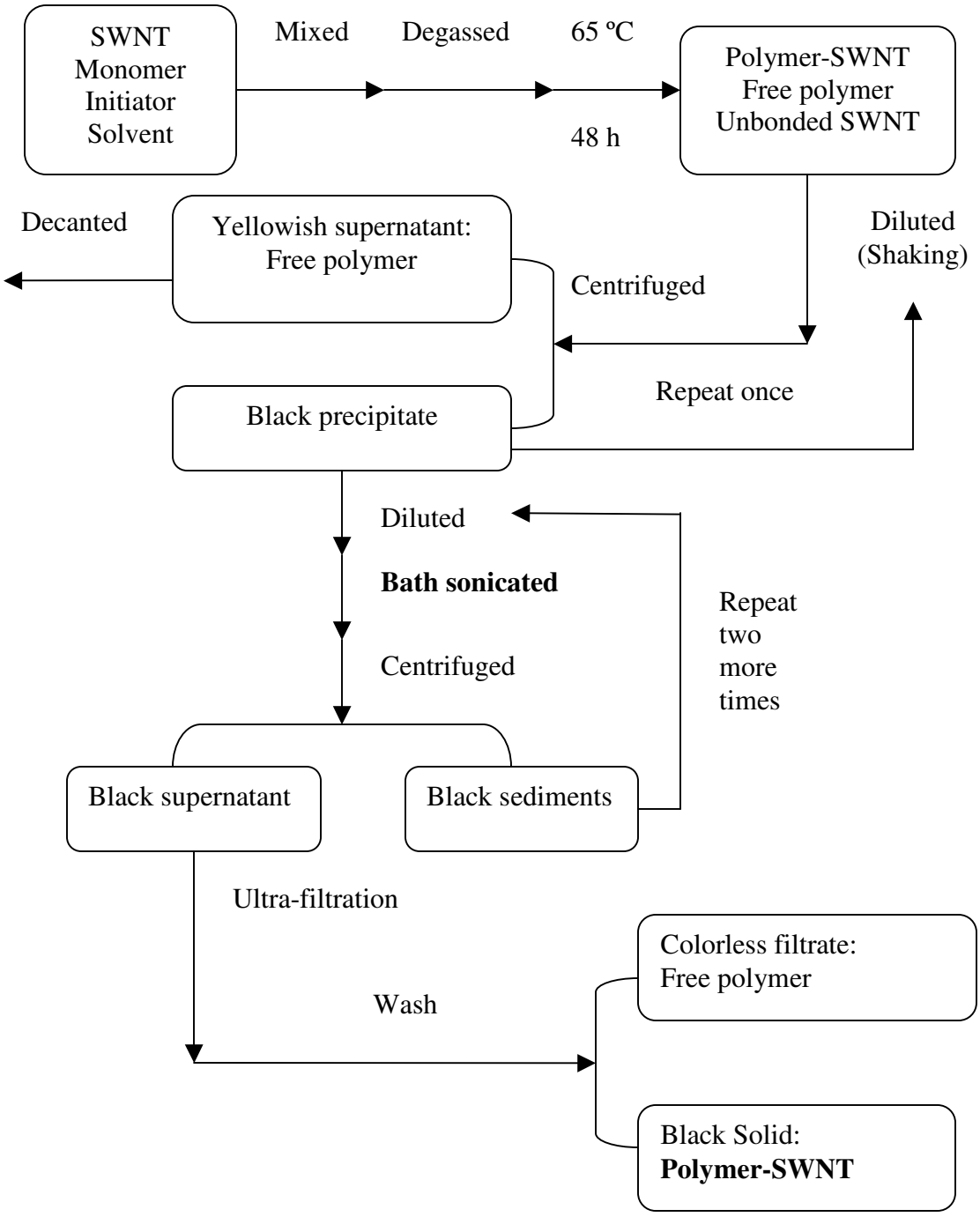

Appendix 2. Transmission FTIR spectra of pristine SWNT, PS and PS-SWNT

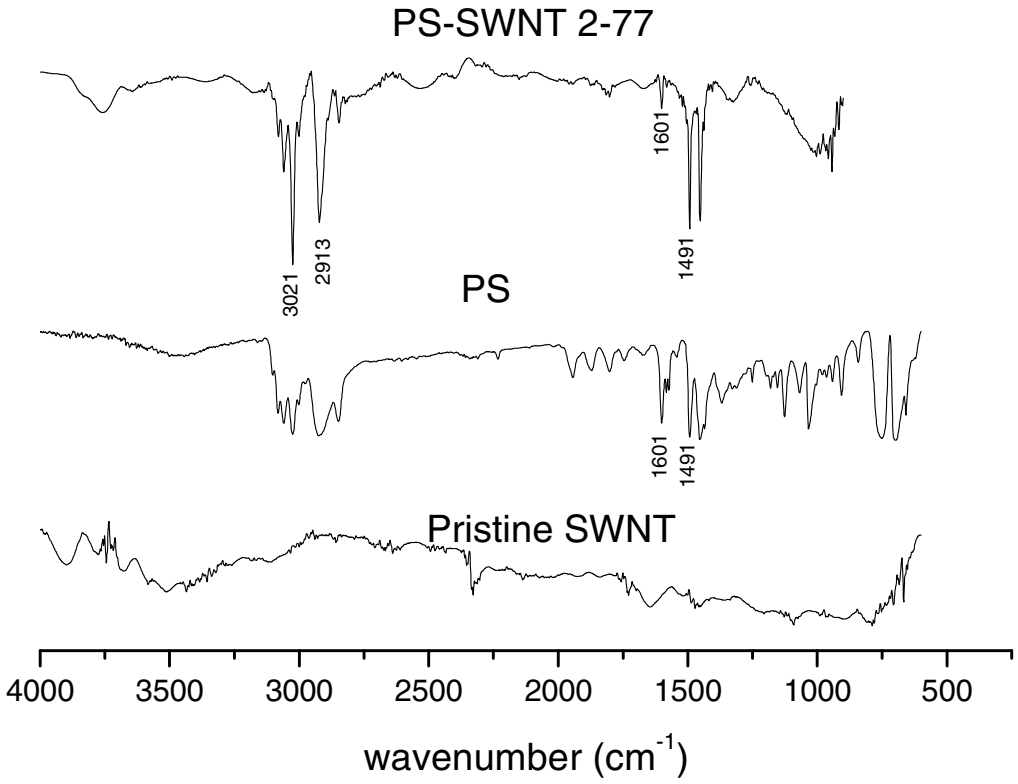

Appendix 3. Transmission FTIR spectra of pristine SWNT, PtBA and PtBA-SWNT

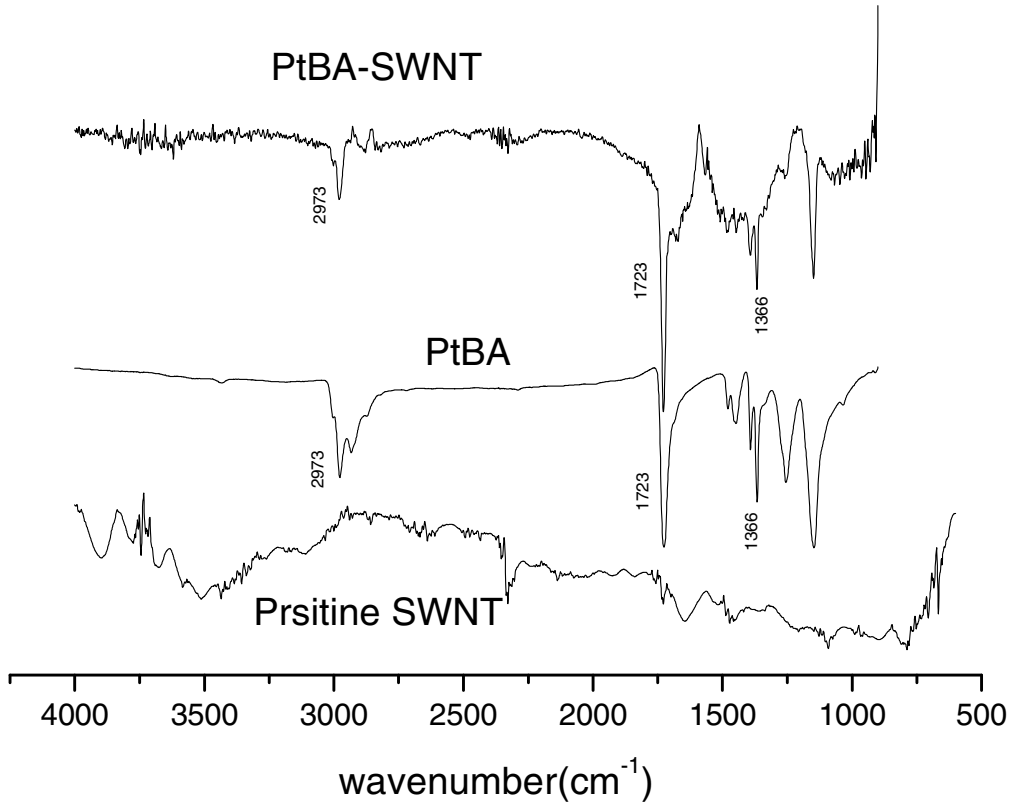

Appendix 4. Transmission FTIR spectra of pristine SWNT, copolymer and copolymer-SWNT

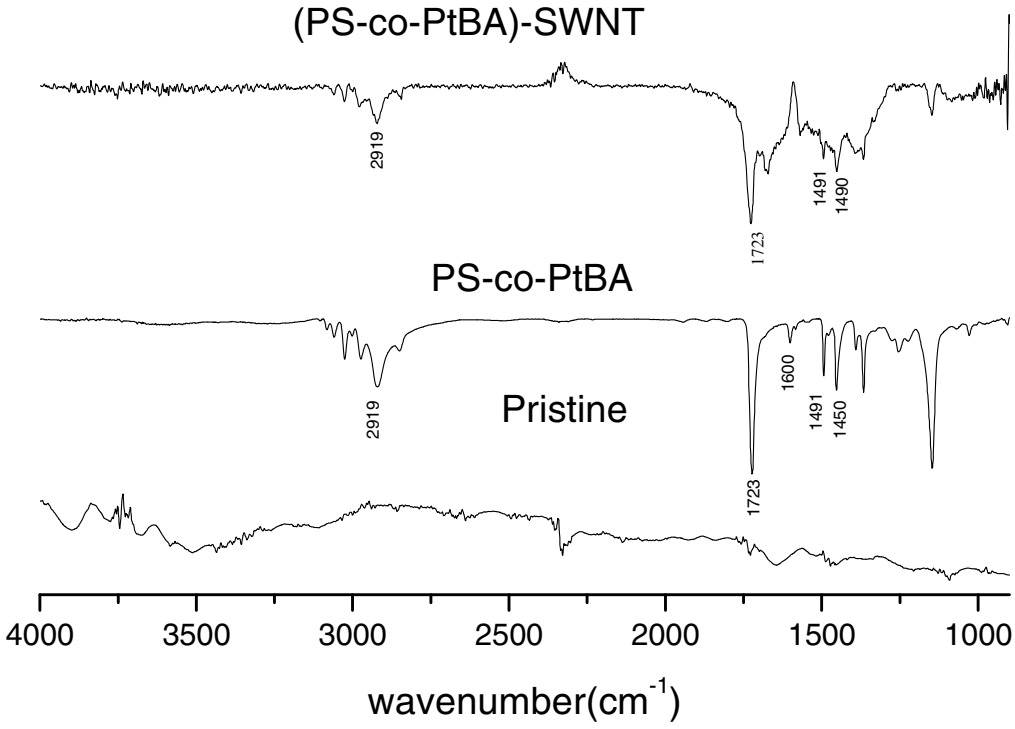

VITA

Xiaoming Jiang

Candidate for the Degree of

Master of Science

Thesis: GRAFTING POLYMERS TO SINGLE-WALLED CARBON NANOTUBES

Major Field: Chemistry

Biographical:

Education: Graduated in Nanjing High School, Jiangyin, China, in July, 1993. Received Bachelor of Engineering in Nanjing University of Technology, China, in July, 1997. Received Master of Engineering in Nanjing University of Technology, China, in July, 2002. Completed the Requirements for the Master of Science degree at Oklahoma State University in July, 2005.

Experience: Employed as an assistant engineer by Jiangyin Power Plant from July, 1997 to August, 1999. Employed as a teaching assistant by Department of Chemistry, Oklahoma State University from August, 2002 to August, 2005.

Name: Xiaoming Jiang Date of Degree: July, 2005

Institution: Oklahoma State University Location: Stillwater, Oklahoma

Title of Study: GRAFTING POLYMERS TO SINGLE-WALLED CARBON NANOTUBES

Pages in Study: 47 Candidate for the Degree of Master of Science

Major Field: Chemistry

Scope and Method of Study: The purpose of this study is to prepare stable dispersed single-walled carbon nanotubes (SWNT) samples and fabricate layer-by layer films from polyelectrolyte-functionalized SWNT solutions. We use in situ free radical polymerization to attach polymer chains to the SWNT, and under sonication, those polymer chains help break large bundles of SWNT into small bundles and make stable black solutions.

Findings and Conclusions: Stable dispersions of PS-SWNT in DMF, PtBA-SWNT in DMF, (PS-co-PtBA)-SWNT in DMF, and PNaA-SWNT in water were obtained by in situ free radical polymerization. AFM images show big bundles were broken into small ones after functionalization, and Raman spectra indicate covalent functionalization of sidewalls of SWNT from increase of D-band intensity with respect to G-band intensity.

ADVISER'S APPROVAL: _____